COBEM 2021 26th International Congress of Mechanical Engineering
November 22-26, 2021, Virtual Congress, Brazil

COB-2021-1070
A SIMPLIFIED MATHEMATICAL MODEL TO PREDICT THE HUMAN BREAST THERMAL RESPONSE

Carlos Dalmaso Neto
Universidade Federal do Paraná
dalmasont@gmail.com

Yasmin Pereira Buabssi
Universidade Federal do Paraná
ybuabssi@gmail.com

José Viriato Coelho Vargas
Universidade Federal do Paraná
vargasjvcv2@gmail.com

Wellington Balmant
Universidade Federal do Paraná
wbalmant@gmail.com

André Bellin Mariano
Universidade Federal do Paraná
andrebmariano@gmail.com

Abstract. *This study produced a simplified tridimensional (3-D) mathematical model to predict the human breast thermal response directly from physical laws and making use of mass, heat, and fluid flow empirical and theoretical correlations. The breast mathematical models described in the literature do not consider blood flow which was included in the proposed model, aiming at an accurate representation of human breast tissues. For that, the human breast was divided in Volume Elements (VE). Each VE accounted for blood perfusion and was assumed to contain a homogeneous mass of tissue with uniform properties, interacting energetically with neighboring elements, thorax, and ambient. Therefore, the model produced a system of ordinary differential equations to calculate the breast internal and surface temperature distributions as functions of time, space (from the imposed VE mesh), and known initial and boundary conditions. The actual breast external shape was taken from the subject photograph and converted into a STL file to produce the computational domain boundaries and mesh, and the breast internal structure was assumed to be known (e.g., from computerized tomography) which includes possible nodules and lumps. The model equations were integrated in time until steady state. The obtained breast surface temperature was compared to the actual breast infrared image temperature distribution with good qualitative agreement. After experimental validation, the model is expected to become a useful tool to study the thermal behavior of the human breast with cancer and possibly accurate early-stage cancer diagnosis and tumor depth prediction.*

Keywords: *temperature field, early-stage cancer diagnosis tool, model adjustment, model experimental validation, Volume Element Method (VEM)*

1. INTRODUCTION

Early diagnosis of breast cancer is, today, the most important action modern medicine has to decrease female mortality rates – 2.1 million cases and 627 deaths in 2018 (INCA, 2019) – as mortality from breast cancer is mainly linked to access to diagnosis and adequate treatment in a timely manner. Ultrasonography and mammography are the elected imaging method in the diagnostic investigation of suspected breast changes, and both methods are seen as complementary in addressing different clinical situations (INCA, 2015).

After screening suspected cases, better classification and confirmation of this tumor is needed, and other image analysis methods can be used, such as magnetic resonance imaging or tomography (INCA, 2015), in order to provide anatomical information about the tumor. Biopsies are used for correct staging, and diagnostic or therapeutic surgical procedures, as well as radiotherapy or chemotherapy, as needed. As stated by Morais et al. (2016), most breast tumors are invasive and can infiltrate other tissues. Breast tumor malignancy is strongly influenced by staging, that is, the extent of the tumor or it's spread when diagnosed early.

Thermographic infrared image is a non-anatomical method that aims to identify vascular changes with greater blood flow and metabolic activity in the breasts that may be related to abnormalities, even when changes are not yet present in other exams (Brioschi, 2016), as the human body is an efficient heat radiator, despite pigmentation or skin color, providing means for a non-invasive investigation method as thermography (Bird; Ring, 1978; Ring, 1977 and Ring; Cosh, 1968).

The observation that a breast cancer can produce an increase in infrared emission, causing disparity in the thermographic pattern of the breast skin, initiated the development of medical thermography (Isard et al., 1972). Gautherie; Gros (1980) states that the rate of cancer detection in reviews of women who were initially considered healthy or with benign mastopathies by methods other than thermography was significantly higher in altered thermography, and that the superficial thermal pattern of the breasts is actually related to the metabolism and vascularization of the underlying tissues (Gautherie, 1980). The abnormalities observed in the thermal behavior of breast neoplasms are due to the excessive vasodilation caused by nitric oxide originating from neoplastic lesions (Anbar et al., 2001), that is, the changes found in breast thermography are due to autonomic responses to histochemical changes occurring at the disease site.

The blood perfusion is important, as the tumor perfusion varies drastically depending of the tumor (Paruch. 2020), and it play an important role in the complex process of female breast cancer evaluation (Gas et al., 2020).The geometric center of a breast tumor localization from its surface temperature could be estimated (Dalmaso Neto et al., 2021). Figueiredo et al. (2019, 2020) demonstrated that the geometric centers of the tumors could be estimated with a maximum error of 0.15 cm in relation to the original location.

To estimates this localization, a methodology based in infrared image in association with tomography, magnetic resonance or ultrasonography will be developed. To this, it is proposed a) a mathematical model that accounts for the blood flow to predict thermal response of human breast; b) develop a software that integrates those images and the mathematical model, to determine breast tumor characteristics and c) evaluate application potential by case studies and possible experimental validation of the model.

2. MATERIALS AND METHODS

2.1 Mathematical modelling

A mathematical model was developed to predict the steady state thermal response of the human breast based on the Volume Elements Model (Dilay et al., 2015 and Vargas et al., 2001), a simplified physical model of the thermal response, where the domain of interest is three-dimensionally discretized using finite volumes with centered cells, and principles of Classical Thermodynamics and Heat Transfer for each cell is applied, resulting in a system of Differential Ordinary Equations in relation to time, using empirical and analytical correlations to quantify the energy interactions between cells. Convergence is obtained with sparse meshes and low computational time for the solution fields in relation to time and space (Dilay et al., 2015, 2017)

The breast VEM discretization consists of dividing the domain into Volume Elements (VE), which are finite volumes centered on cubic cells (Figure 1), containing fluid inside them – being health tissue, tumoral tissue, and blood. As a result, the system's spatial dependence is incorporated into the model. Through the formulation of a speed field in the domain, an Ordinary Differential Equation with respect to time is derived to calculate the quantity of interest, in this case the temperature, in each VE, and all the VE interacts energetically with each other. Temperature measurements available in selected cases was used to undermine the breast tumor possible localization. For this, tomography, resonance or ultrasonography image was used to establish thermophysical proprieties of the breast.

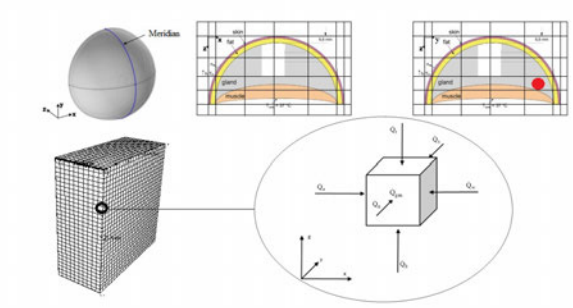

Figure 1. 3D view of the breast hemispheric model. Cuttings on the x-z and y-z plans, with the discretized mathematical domain and the energy interactions in a Volume Element (VE)

Mass conservation in any volume element indicates that:

$$\frac{d(\rho V)_i}{dt} = \sum_{j=e,w,t,b,n,s} \left(\dot{m}_{in,j} - \dot{m}_{out,j} \right) \quad (1)$$

where ρ is density, V is volume, t is time and $\dot{m}$ the mass flow rate *in* or *out* the face *j* of the volume element. Assuming constant volume and incompressible flow, $d(\rho V)_i / dt = 0$.

The mass flow rates are estimated based on the average blood perfusion in each VE (Vargas et al., 2005). assuming that in half of the area of each face of the VE, the blood flow enters the VE and, therefore, in the other half an identical flow exits the VE, thus satisfying the conservation of the mass on each face of all the VEs that make up the breast human. In this way, the approximate mass flow of blood perfusing the breast was established.

Next, the principle of energy conservation applied to all VEs stated that:

$$\frac{dT_i}{dt} = \frac{1}{(\rho V c)_i}\left(\sum_{j=e,w,t,b,n,s} \dot{Q}_j + \dot{Q}_{gen} \right)_i \tag{2}$$

where T is temperature, t is time, c is the specific heat, Q accounts for heat transfer modes by convection, conduction, radiation (where applicable, such as on top or side walls under sun exposure), and Q_{gen} is internal heat generation terms.

The VEM allows the existence, in the same computational domain, of three types of elements: **solid**, **fluid** and **mixed**. It is possible that all types of elements coexist in an integrated way within the same region of the computational domain (Dilay et al., 2015, 2017). For any possible interaction, the appropriate equation for each type of interaction must be written. Possible interactions are: a) Solid and Solid VE; b) Solid and Fluid VE; c) Solid and Mixed VE; d) Fluid and Fluid VE; e) Fluid and Mixed VE; f) Mixed and Mixed VE; g) Solid VE and computational domain boundary; h) Fluid VE and computational domain boundary; and j) Mixed VE and computational domain boundary. In this mathematical modeling of the breast, the Fluid Volume Element was chosen to represent the living tissue.

2.2 Breast Three-dimensional Modeling

To reproduce the outline of the human breast, a 3D model was constructed from an MRI image. An image of a 50-year-old female patient was used. The MRI scan provides files in the DICOM standard, which contain all serially sliced images. For the thermal simulation of the breast, a 3D model in STL ("standard triangle language") is required, a file format for three-dimensional information, which will later receive a cubic mesh. The three-dimensional geometry was generated using Invesalius 3.31 software, as shown in Figure 2

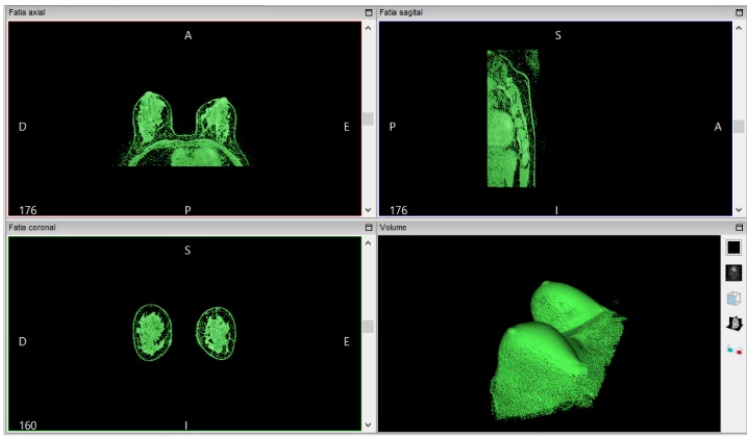

Figure 2. 3D breast reconstruction using Magnetic Resonance Image

Based on the set of two-dimensional MRI images, **Invesalius** reconstructs the body region in three dimensions, and separates the tissues into editable masks. This is possible from the gray scale of the exam, which relate to the radiodensity of the tissues examined (Valente, 2008).

Despite being very close to the real shape of the human breast, the result obtained in STL (Figure 3A) contains a series of unwanted noises, such as the contour of the stretcher, which can make it difficult to apply the cubic mesh. Therefore, **MeshMixer** software was used to clean all imperfections, and smooth the model surface. The 3D Model obtained is a faithful contour of the human breast, which ensures better precision and integrity in the simulation results. Even so, it ensures simplicity to the computational domain. The result can be seen in Figure 3B.

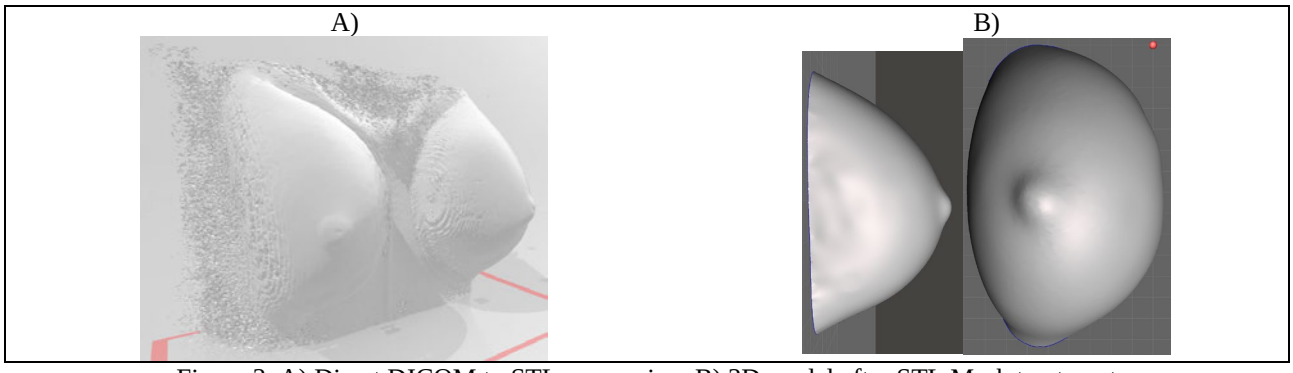

Figure 3. A) Direct DICOM to STL conversion. B) 3D model after STL Mesh treatment

Then, the model is discretized using a uniform cubic mesh, each cube being one of the studied volume elements. For a first simulation, 60,000 volume elements were applied in the domain (50 x 30 x 40), as shown in Figure 4. This number was evaluated by numerical convergence tests, seeking to ensure accuracy and low computational time, as explained later.

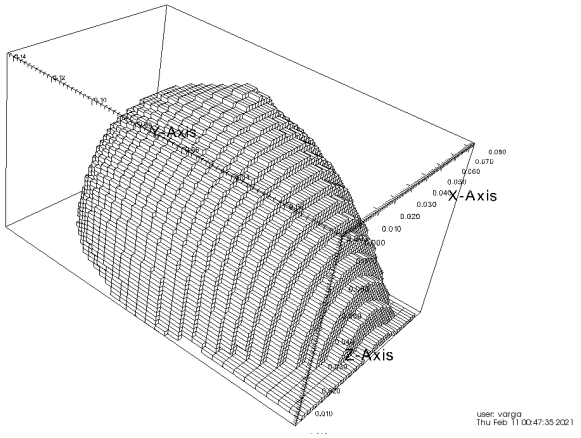

Figure 4. Discretized Computational Domain of the Breast

Finally, for the use of this model discretized in volume elements by the computer program, an additional step involving the three-dimensional model with a box is carried out. Through a process called "ray tracing" (a line originating from the center of each mesh element is drawn in an arbitrary direction and the number of intersections of the line with the vertices is counted. The element is located inside or outside the mesh if the number of intersections is odd or even, respectively) a three-dimensional solid is then delivered, with only the Volume Elements that contain the breast to be simulated, ready for computational analysis. This entire process is schematically represented in Figure 5.

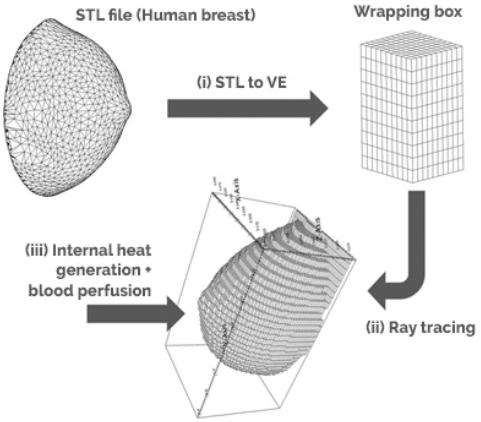

Figure 5. Human breast mesh generation process

2.3 Breast Volume Elements

At all the 6 possible faces, the Volume Element can be in one of the two situations: a) External: where the interaction occurs between the Volume Element (tumoral or healthy) and the breast surface; b) Internal: where the interaction occurs between the Volume Elements (tumoral and tumoral, tumoral and healthy, healthy and tumoral and healthy and healthy). When in External situation, radiation and external convection must be accounted. When in Internal situation, conduction and internal convection must be accounted. A special case is the bottom face, that is in contact with de thoracic wall, as the heat exchanges occur at body temperature. All the possible cases are illustrated in Figure 6.

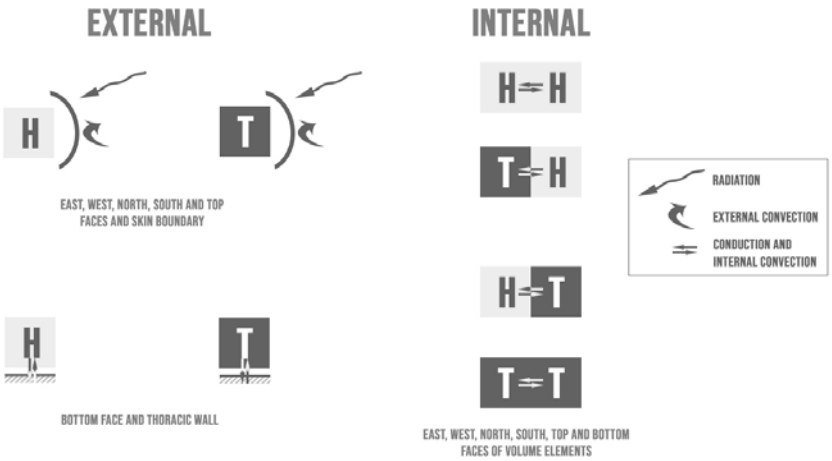

Figure 6. All Breast Volume Elements possible interactions, at the Computational Domain

2.4 Adjustment and Validation of the Mathematical Model

The specific volumetric flow rate of blood in tumor cells is 0.32 mL/min/g, and 0.06 mL/min/g for healthy breast cells (Mankoff et al., 2002). Assuming constant blood density in the breast, the ratio of blood mass flow rates between tumor and healthy cells is estimated by:

$$r_{\mathrm{TH}} = \frac{\dot{m}_{\mathrm{T}}}{\dot{m}_{\mathrm{H}}} = \frac{0,32}{0,06} = 5,33 \tag{3}$$

where $\dot{m}_{\mathrm{T}}$ and $\dot{m}_{H}$ are the blood mass flow rates of a tumor breast tissue, and a healthy breast tissue, respectively, and that cross the faces of a tumor and healthy VE, respectively.

The energy released from the hydrolysis of ATP to ADP is used to carry out cellular work, usually by coupling the exergonic ATP hydrolysis reaction with endergonic reactions. The molecular mass of ATP (m_{ATP}) is 507.18 g/mol. The calculated ΔG for the hydrolysis of 1 mol of ATP is -57 kJ/mol, and the enthalpy change, ΔH , is -24 kJ/mol.

In order to calculate the energy balance in breast tumor cells and normal breast cells in the VE, first calculate the specific Gibbs free energy and the heat of reaction released by ATP hydrolysis in kJ/kg of the as follows:

$$\Delta \mathrm{G} = \frac{\Delta \mathrm{G} \times 10^{3}}{m_{\mathrm{ATP}}} = \frac{-57000}{507,18} \therefore \boxed{\Delta \mathrm{G} = 112,39 \text{ kJ/kg}} \tag{4}$$

$$\Delta \mathrm{H} = \frac{\Delta \mathrm{H} \times 10^{3}}{m_{\mathrm{ATP}}} = \frac{-24000}{507,18} \therefore \boxed{\Delta \mathrm{H} = 47,32 \text{ kJ/kg}} \tag{5}$$

Then, the mass flow of blood entering and leaving through the j faces of each VE is estimated as follows:

$$\dot{m}_{\mathrm{BLH,in},j} = \dot{m}_{\mathrm{BLH,out},j} = \rho_{BL} u_j \frac{\mathrm{A}_j}{2} \tag{6}$$

where $\dot{m}_{\mathrm{BLH,in,j}}$ and $\dot{m}_{\mathrm{BLH,out,j}}$ are the mass flow rates of blood from healthy breast tissue, which enter and exit face j of the VE, respectively.

Also, u_{j} is the average velocity of blood that crosses the face of the VE both entering and exiting. This velocity is estimated from the typical volumetric flow pumped by a human heart for each breast, $\dot{\forall}_{BL} \simeq 6$ L/m (VARGAS et al., 2005). Thus, considering half of the individual's breast base area known, $A_{bm}/2$, and applying mass conservation, we obtain $u_j = \dot{\forall}_{BL} / (A_{bm}/2)$.

Next, $\dot{m}_{\mathrm{BLT,in,j}} = \dot{m}_{\mathrm{BLT,out,j}} = r_{TH} \times \dot{m}_{\mathrm{BLH,in,j}}$ is estimated as the mass flow rates of blood from a breast tumor tissue, which enter and exit through face j of the VE, respectively, using the r_{TH} ratio calculated in Eq. (3)

Next, calculate the heat transfer rate by convection (q_{conv})across the VE faces as follows:

a) Let the volume element be a mammary tumor cell (T):

$$\mathrm{VE_T} \rightarrow \dot{q}_{\mathrm{conv,j}} = \dot{m}_{BLT,in,j}[\mathrm{kg/s}] \times c_{\mathrm{BL}} \times (\mathrm{T_{IN}} - \mathrm{T_{OUT}}) \tag{7}$$

b) Let the volume element be a normal breast cell (H):

$$\mathrm{VE_H} \rightarrow \dot{q}_{\mathrm{conv,j}} = \dot{m}_{BLH,in,j}[\mathrm{kg/s}] \times c_{\mathrm{BL}} \times (\mathrm{T_{IN}} - \mathrm{T_{OUT}}) \tag{8}$$

where $\mathrm{T_{IN}}$ is the inlet temperature and $\mathrm{T_{OUT}}$ the outlet temperature.

Finally, we use Eq. (7) and Eq. (8) to estimate the rate of heat generation in the VE, assuming an ATP consumption rate per volume unit according to a constant to be calibrated, $c_{\mathrm{ATP}}[\mathrm{kg/s/m^3}]$. This is physically explained by the fact that the blood brings nutrients to the cells that are needed to produce ATP in the Krebs Cycle. Therefore, the Heat Generation Rate – assuming 1×10^7 W/m^3 and 2×10^4 W/m^3 for tumor and healthy tissues (Lozano et al., 2020), respectively – is estimated as follows:

a) Let the volume element be a mammary tumor cell (T):

$$\dot{q}_{\mathrm{gen}}[\mathrm{W/m^3}] = c_{\mathrm{ATP_T}}[\mathrm{kg/s/m^3}] \times \mathrm{V_{VE}}[\mathrm{m^3}] \times \Delta\mathrm{H}[\mathrm{J/kg}] \therefore 1\times10^7 = c_{\mathrm{ATP_T}} \times 47,32 \therefore \boxed{c_{\mathrm{ATP_T}} = 211,33 \ \mathrm{kg/s/m^3}} \tag{9}$$

where $c_{\mathrm{ATP_T}}$ is the rate of ATP consumption per unit volume estimated for a tumor cell.

b) Let the volume element be a normal breast cell (H):

$$\dot{q}_{\mathrm{gen}}[\mathrm{W/m^3}] = c_{\mathrm{ATP_H}}[\mathrm{kg/s/m^3}] \times \mathrm{V_{EV}}[\mathrm{m^3}] \times \Delta\mathrm{H}[\mathrm{J/kg}] \therefore 2\times10^4 = c_{\mathrm{ATP_H}} \times 47,32 \therefore \boxed{c_{\mathrm{ATP_H}} = 0,423 \ \mathrm{kg/s/m^3}} \tag{10}$$

where $c_{\mathrm{ATP_H}}$ is the rate of ATP consumption per unit volume estimated for a healthy cell.

To start the simulations, $c_{\mathrm{ATP_T}}$ and $c_{\mathrm{ATP_H}}$ are assumed based on literature values. The constants $c_{\mathrm{ATP_T}}$ and $c_{\mathrm{ATP_H}}$ are parameters to be adjusted by solving the inverse parameter estimation problem (Minkowycz et al., 2006), using infrared imaging measurements of the breast surface.

$$\frac{c_{\mathrm{ATP_T\ Adjusted}}}{c_{\mathrm{ATP_T}}} = \frac{\mathrm{T_{Thermography}}}{\mathrm{T_{Simulation}}} \tag{11}$$

$$\frac{c_{ATP_H\ Adjusted}}{c_{ATP_H}} = \frac{T_{Thermography}}{T_{Simulation}} \tag{12}$$

With the use of Eq. (11) and Eq. (12) the values of $c_{ATP_T\ Adjusted}$ and $c_{ATP_H\ Ajusted}$ were obtained, used in the simulations of real cases, and the inverse problem was solved.

2.5 Computational Software and Thermal Simulation Results

The system of equations was integrated in time using Runge-Kutta/Felhberg method, with given initial conditions and adaptative step control to control Local Truncation Error ($\leq 10^{-4}$). A condition was defined in which the norm of the temporal derivative of the vector with all variables been integrates ($\leq 10^{-3}$). The system could be resolved directly to the steady state solution, as the transient solution was not of concern, and the unknowns are the stationary temperatures at the center of each volume element. Then the nonlinear system resulting from the algebraic equations was solved using the Newton-Raphson method, and the system was linearized with respect to the unknown value at the center of the cell. These methods were programmed using FORTRAN language. The convergence of numerical results was verified by successive refinements of the mesh, with monitoring of the variation in the Euclidean norm of the numerical solution for the entire domain (≤0,01). For image processing, the files with numerical temperature results were used by the public domain VisIt application, made available by Lawrence Livermore Laboratory (Childs et al., 2012).

3. RESULTS AND DISCUSSION

3.1 SIMULATION WITH LITERATURE DATA ENTRY

The first simulation was performed with literature data. Figure 7A shows the results using calculated $c_{ATP_T} = 211,33\ kg/s/m^3$ and $c_{ATP_H} = 0,423\ kg/s/m^3$, arbitrary coordinates (x=0,04; y=0,04; z=0,04) and dimensions 0.001m, with resulting heat distribution in simulated breast. In frontal view (Figure 7B) it can be seen a focal area on top hemisphere of the breast, as result of the heat transfer from the simulated nodule inside, with 35.6 °C. And X, Y and Z axis intercepting the simulated nodule geometric center where performed (Figure 7C, D and E). This first simulation lasted 259 seconds, and demonstrated that the process is capable to simulate a nodule.

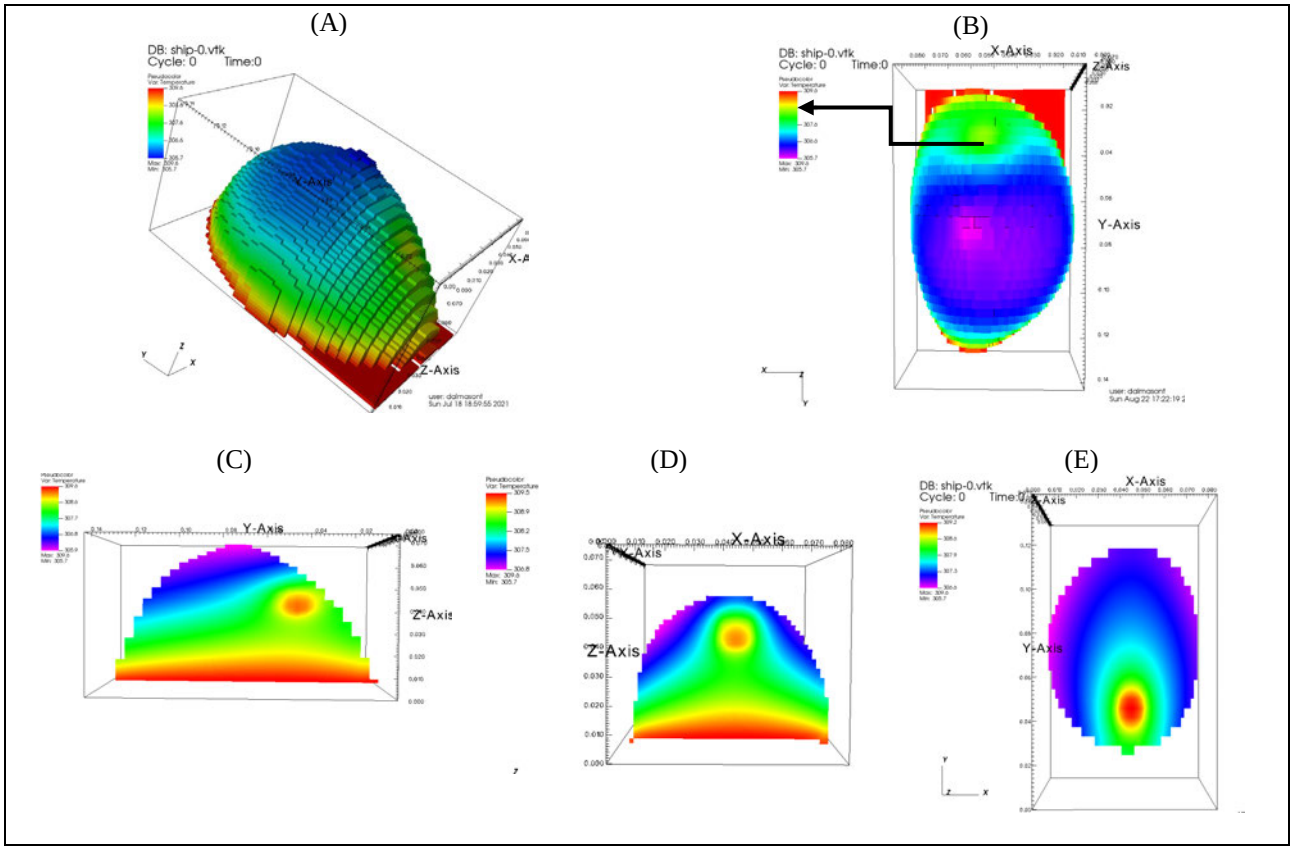

Figure 7. Temperature field od the breast obtained by simulation

3.2 MATHEMATICAL MODEL ADJUSTMENT

In order to adjust c_{ATP_T} and c_{ATP_H}, it must be used a real infrared image of breast cancer, confirmed by biopsy, in a spot similar of the simulated nodule. The breast ultrasonography of a 35-year-old female breast describes a nodule of 3.4x2.1x3.9cm, upper lateral quadrant, 1.32cm deep. 34.0°C was measured as maximum temperature in breast surface.

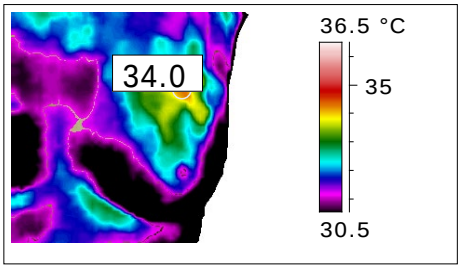

Figure 8. Breast thermography

As in the simulation the surface temperature as 35.6°C, the linear adjustment proposed in was performed as follows:

$$\frac{c_{ATP_T\ Adjusted}}{c_{ATP_T}} = \frac{34,0^{\circ}C}{35,6^{\circ}C} \therefore \frac{c_{ATP_T\ Adjusted}}{211,33} = \frac{34,0^{\circ}C}{35,6^{\circ}C} \therefore \boxed{c_{ATP_T\ Adjusted} = 201,832\ kg/s/m^3} \quad (13)$$

$$\frac{c_{ATP_H\ Adjusted}}{c_{ATP_H}} = \frac{34,0^{\circ}C}{35,6^{\circ}C} \therefore \frac{c_{ATP_H\ Adjusted}}{0,423} = \frac{34,0^{\circ}C}{35,6^{\circ}C} \therefore \boxed{c_{ATP_H\ Adjusted} = 0,404\ kg/s/m^3} \quad (14)$$

Using adjusted c_{ATP_T} e c_{ATP_H} and the given localization, a new simulation as performed (Figure 9). This time, the temperature simulated was the same as the measured in thermography. Simulation lasted 301 seconds.

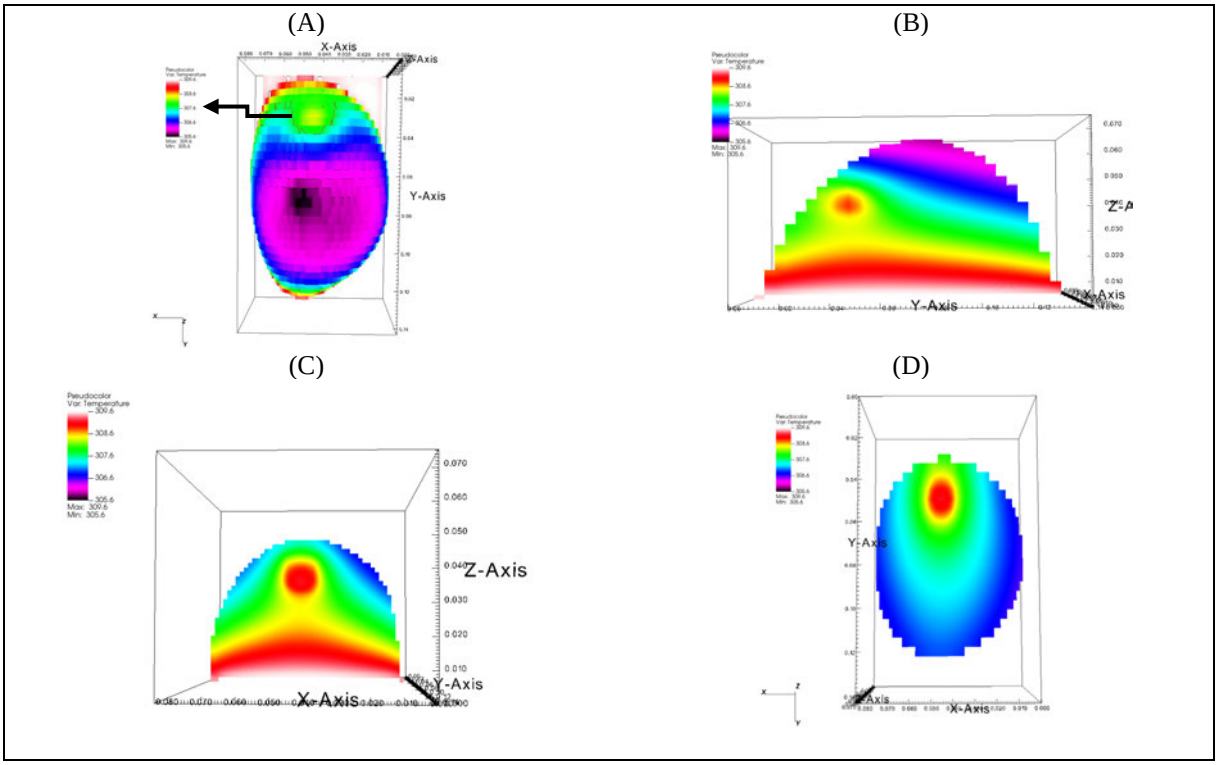

Figure 9. New simulation with adjusted constants. (A) Frontal view; (B)X axis; (C) Y axis; (D) Z axis

3.3 MATHEMATICAL MODEL EXPERIMENTAL VALIDATION

3.3.1 LOWER LATERAL RIGHT BREAST QUADRANT NODULE

Simulation of a nodule of 2.0 x 0.9 x 1.7 cm, in lower lateral right breast quadrant, 4.7cm deep, as described in breast tomography, is showed in Figure 10A. Both simulated and infrared thermography nodule surface temperature was 34.6°C. Figure 10B shows the infrared thermography of the breast with the nodule, biopsy confirmed cancer. Figure 10C, D and E show X, Y and Z axis, demonstrating the tumor localization. The simulation lasted 332seconds.

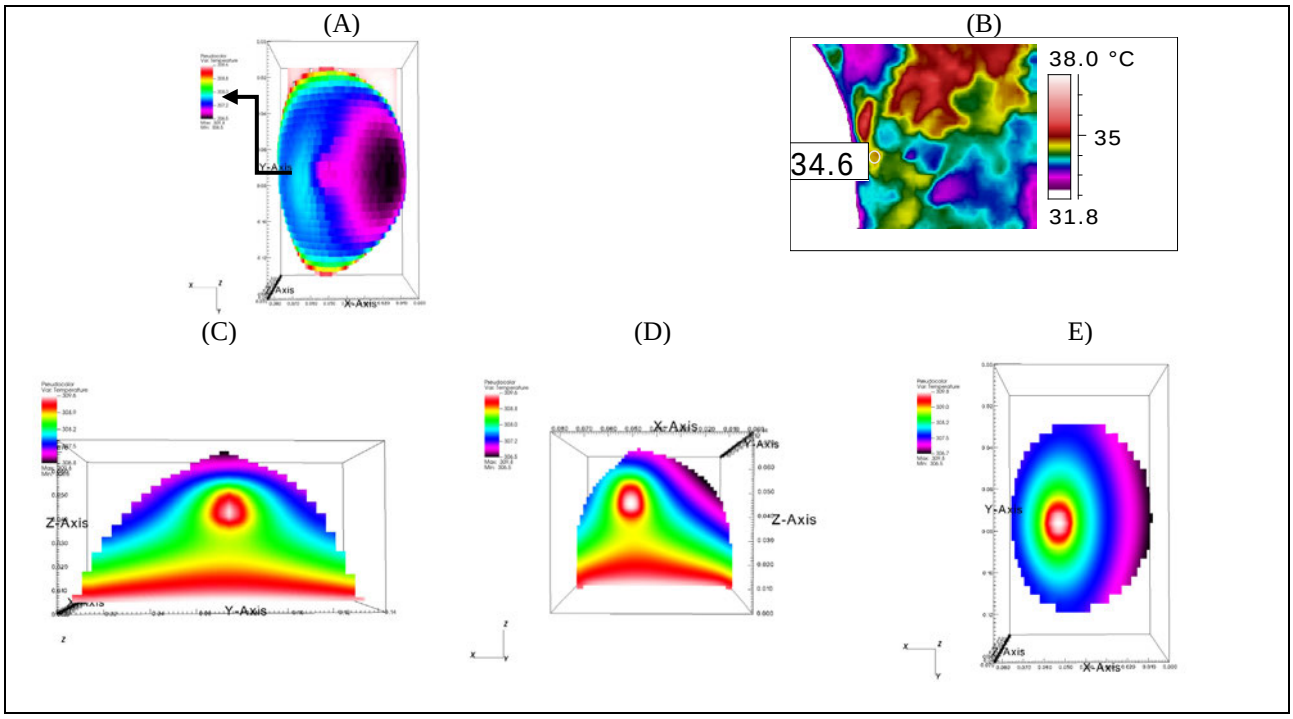

Figure 10. (A) Simulated breast; (B) Infrared image of the breast; (C)X axis; (D) Y axis; (D) Z axis

3.3.2 UPPER MEDIAL LEFT BREAST QUADRANT NODULE

Simulation of a nodule of 1.14 x 0.72 x 1 cm, in upper medial left breast quadrant, 0.4cm deep, as described in breast magnetic resonance image, is showed in Figure 11A. Both simulated and infrared thermography nodule surface temperature was 34.4°C. Figure 11B shows the infrared thermography of the breast with the nodule, biopsy confirmed cancer. Figure 11C, D and X, Y and Z axis, demonstrating the tumor localization in simulation, that lasted 299 seconds.

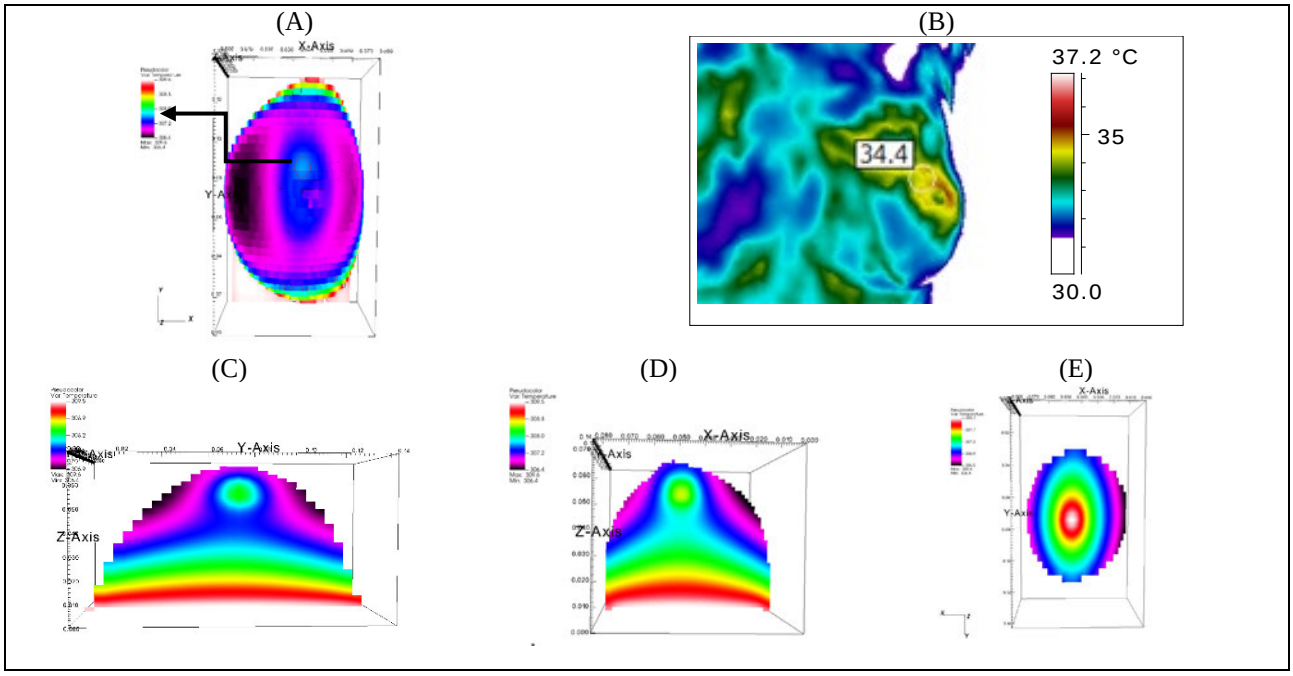

Figure 11. (A) Simulated breast; (B) Infrared image of the breast; (C)X axis; (D) Y axis; (D) Z axis

3.4 SIMULATION OF TWO NODULES IN SAME BREAST

Simulation of a nodule of 1.66 x 1.77 x 1.43 cm, 0.45cm deep, and a nodule of 1.86 x 1.13 x 1.54 cm, 0,4mm deep, both on right breast lateral quadrant, are showed in Figure 12A. Both simulated and infrared thermography nodule surface temperature was 36.3°C. Figure 12B shows the infrared thermography of the breast with the aforementioned nodule, biopsy confirmed cancer. Figure 12C, D and E show X, Y and Z axis, demonstrating the tumor localization. The simulation lasted 354 seconds.

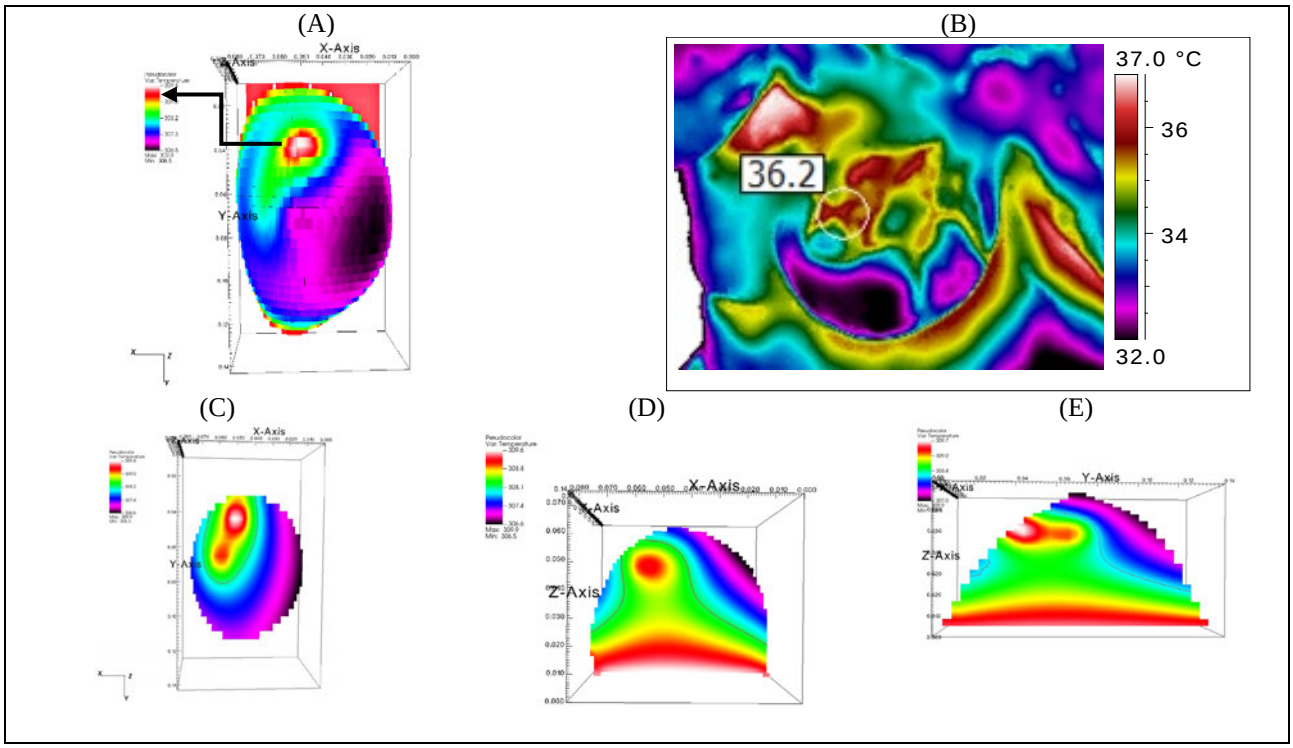

Figure 12. (A) Simulated breast; (B) Infrared image of the breast; (C)X axis; (D) Y axis; (D) Z axis

3.5 DISCUSSION OF METHOD POTENTIAL APPLICATION

Since it was possible to experimentally validate the proposed mathematical model for the human breast, precision and low computational time are expected due to the use of the volume element method. Thus, the proposed methodology is to use infrared imaging and anatomical imaging exams for possible diagnosis of benign or malignant growths in the human breast.

A possible approach would be to assume that growths present in the anatomical exams are malignant in order to perform the computational simulation of the thermal response of the breast, internal and superficial, with the application proposed in this work. With the available simulated surface temperature distribution, it is possible to perform the comparison with an infrared image of the same breast. In this way, if there is a qualitative and quantitative agreement between the simulation and the infrared image temperatures, it is expected that the growth will be malignant. If the infrared image shows temperatures significantly different and lower than the surface temperature distribution obtained by the simulation, the growth is expected to be benign.

4. CONCLUSION

A methodology based in infrared image, associated to anatomical image exams was developed to locate breast tumors. The main conclusions are: 1) a mathematical model to predict breast thermal response was developed; 2) Thermophysical characteristics were determined and a mathematical model as proposed, using Volume Elements Method; 3) A software which integrates anatomical and infrared images was developed, and, by means of case studies, established it application and precision; 4) The potential application of the method was evaluated through the study of 4 cases, with the validation of the data being achieved, and with the use of the method in the evaluation of more than one tumor in the same breast, with success; and 5) As proposed in the discussion, the comparison of breast surface temperatures obtained by simulation and by infrared imaging has the potential to make the diagnosis of malignant or benign breast growth.

The method opens up opportunities for simulations in other areas of the body. One region that has a similar conformation is the thyroid. The study of limits for amputations, the study of brown fat metabolism, among others, are other candidates for simulation with the Volume Elements Method that should be done in future opportunities.

5. ACKNOWLEDGEMENTS

To the Brazilian National Council of Scientific and Technological Development, CNPq (projects 407198/2013-0, 403560/2013-6, 407204/2013-0, 430986/2016-5, 443823/2018-9, 313646/2020-1, 310708/2017-6, 308460/2020-0 and 446787/2020-5), CAPES, Ministry of Education, Brazil (projects 062/14 and CAPES-PRINT-UFPR-88881.311981/2018-01), and Araucaria Foundation of Parana, Brazil (project 115/2018, no. 50.579 – PRONEX).

6. REFERENCES

Anbar, M.; Milescu, L.; Naumov, A.; et al., 2001. *Detection of cancerous breasts by dynamic area telethermometry*. IEEE Engineering in Medicine and Biology Magazine, v. 20, n. 5, p. 80–91.

Bird, H. A.; Ring, E. F. J., 1978. *Thermography and radiology in the localization of infection*. Rheumatology, v. 17, n. 2, p. 103–106.

Brioschi, M. L., 2016. *Diagnóstico precoce de Câncer de Mama não tem Clínica: Estudo combinado por Termografia*. Pan American Journal of Medical Thermology, v. 3, n. 1, p. 19–24.

Childs, H.; Brugger, E.; Whitlock, B.; et al., 2012. *VisIt: An End-User Tool For Visualizing and Analyzing Very Large Data*. High Performance Visualization--Enabling Extreme-Scale Scientific Insight. p.357–372.

Dalmaso Neto, C.; Vargas, J. V. C.; Brioschi, M. L., 2021. *Infrared imaging and computerized tomography in breast cancer: case study*. RETERM - Thermal Engineering.

Damasceno, B.; Figueiredo, A., 2020. *ANÁLISE NUMÉRICA DA TERMOGRAFIA DINÂMICA PARA DETECÇÃO PRECOCE DO CÂNCER DE MAMA*. XXVII Congresso Nacional de Estudantes de Engenharia Mecânica. **Anais...** . ABCM.

Dehlinger, L., 2004. *The MRI Inventors: Who Was Responsible?*. Essai, v. 2, n. 9.

Delestri, L. F. U.; Ito, K.; Seng, G. H.; Shakhih, M. F. M.; Wahab, A. A., 2020. *Thermal profiling analysis for asymmetrically embedded tumour with different breast densities*. Malaysian Journal of Medicine and Health Sciences, v. 16, n. September, p. 6–12.

Dilay, E.; Vargas, J. V. C.; Souza, J. A.; et al., 2015. *A volume element model (VEM) for energy systems engineering*. International Journal of Energy Research, v. 39, n. 1, p. 46–74.

Dilay, E.; Vargas, J. V. C.; Souza, J. A.; et al., 2017. *Modelagem e simulação para engenharia de sistemas*. In: J. V. C. Vargas; L. K. Araki (Orgs.); Cálculo Numérico Aplicado. 1º ed, p.475–556. Manole.

Ferreira, M.; Yanagihara, J., 2011. *Um modelo do sistema termorregulador do corpo humano: exposição a ambientes quentes*. Research on Biomedical Engineering, v. 15, n. 1–2, p. 87–96.

Figueiredo, A. A. A.; Fernandes, H. C.; Guimaraes, G., 2018. *Experimental approach for breast cancer center estimation using infrared thermography*. Infrared Physics and Technology, v. 95, n. October, p. 100–112. Elsevier.

Figueiredo, A. A. A.; Fernandes, H. C.; Malheiros, F. C.; Guimaraes, G., 2020. *Influence analysis of thermophysical properties on temperature profiles on the breast skin surface*. International Communications in Heat and Mass Transfer, v. 111, p. 104453.

Figueiredo, A. A. A.; Do Nascimento, J. G.; Malheiros, F. C.; et al., 2019. *Breast tumor localization using skin surface temperatures from a 2D anatomic model without knowledge of the thermophysical properties*. Computer Methods and Programs in Biomedicine, v. 172, p. 65–77.

Gas, P.; Miaskowski, A.; Dobrowolski, D., 2020. *Modelling the tumor temperature distribution in anatomically correct female breast phantom*. Przeglad Elektrotechniczny, v. 96, n. 2, p. 146–149.

Gautherie, M., 1980. *Thermopathology of Breast Cancer: Measurement and Analysis of in vivo temperature and blood flow*. Annals of the New York Academy of Sciences, v. 335, n. 1 Thermal Chara, p. 383–415.

Gautherie, M.; Gros, C. M., 1980. *Breast thermography and cancer risk prediction.* Cancer, v. 45, n. 1, p. 51–56.

González, F. J., 2021. *Thermal Simulations of Cancerous Breast Tumors and Cysts on a Realistic Female Torso*. Journal of Biomechanical Engineering, , n. c, p. 1–40.

INCA. **Diretrizes para a Detecção Precoce do Câncer de Mama no Brasil**. Rio de Janeiro: INCA, 2015.

INCA. **A situação do câncer de mama no Brasil: síntese de dados dos sistemas de informação.** Rio de Janeiro: INCA, 2019.

Isard, H. J.; Becker, W.; Shilo, R.; Ostrum, B. J., 1972. *Breast thermography after four years and 10,000 studies*. American Journal of Roentgenology, v. 115, n. 4, p. 811–821.

Lozano, A.; Hayes, J. C.; Compton, L. M.; Azarnoosh, J.; Hassanipour, F., 2020. *Determining the thermal characteristics of breast cancer based on high-resolution infrared imaging, 3D breast scans, and magnetic resonance imaging*. Scientific Reports, v. 10, n. 1, p. 1–14. Springer US.

Morais, K. C. C.; Vargas, J. V. C.; Souza, G. A. G. R. De; et al., 2016. *An infrared image based methodology for breast*

lesions screening. Infrared Physics & Technology, v. 76, p. 710–721. Elsevier B.V.

Paruch, M., 2020. *Mathematical modeling of breast tumor destruction using fast heating during radiofrequency ablation*. Materials, v. 13, n. 1.

Ring, E. F.; Cosh, J. A., 1968. *Skin temperature measurement by radiometry*. British Medical Journal, v. 4, n. 5628, p. 448–448.

Ring, E. F. J., 1977. *Quantitative Medical Thermography*. In: W. D. Lawson (Org.); SPIE - The International Society for Optical Engineering. **Anais...** . v. 110, p.78–84.

Souza, G. A. G. R. De; Brioschi, M. L.; Vargas, J. V. C.; et al., 2015. *Reference breast temperature: proposal of an equation*. Einstein (São Paulo, Brazil), v. 13, n. 4, p. 518–524.

Valente, L., 2008. *O software para cirurgias InVesalius, desenvolvido por centro de pesquisa, é liberado para uso público*. Ciênc. cult. (São Paulo), p. 8–9.

Vargas, J. V. C.; Brioschi, M. L.; Dias, F. G.; et al., 2008. *Normalized methodology for medical infrared imaging*. Infrared Physics & Technology, v. 52, n. 1, p. 42–47. Elsevier B.V.

Vargas, J. V. C.; Stanescu, G.; Florea, R.; Campos, M. C., 2001. *A Numerical Model to Predict the Thermal and Psychrometric Response of Electronic Packages*. Journal of Electronic Packaging, v. 123, n. 3, p. 200–210.

Vargas, J. V. C.; Vlassov, D.; Colman, D.; Brioschi, M. L., 2005. *A thermodynamic model to predict the thermal response of living beings during pneumoperitoneum procedures*. Journal of Medical Engineering and Technology, v. 29, n. 2, p. 75–81.

Werner, J.; Buse, M., 1988. *Temperature profiles with respect to inhomogeneity and geometry of the human body*. Journal of Applied Physiology, v. 65, n. 3, p. 1110–1118.

7. RESPONSIBILITY NOTICE

The authors are the only responsible for the printed material included in this paper.